American Journal of Materials Research
2014; 1(4): 53-58

ISSN: 2375-3919

American Association for Science and Technology

Keywords
Reinforced Concrete,
Mineral Admixtures,
Corrosion,
Passive Film,
XRD,
SEM

Received: October 08, 2014
Revised: October 18, 2014
Accepted: October 19, 2014

Effect of Al_2O_3 additives on the corrosion and electrochemical behavior of steel embedded in ordinary Portland cement concrete

Mosaad Mohamad Sadawy

Mining and Petroleum Engineering Department, Al-Azhar University, Nasr City, Cairo, Egypt

Email address
mosaadsadawy@yahoo.com

Citation
Mosaad Mohamad Sadawy. Effect of Al_2O_3 Additives on the Corrosion and Electrochemical Behavior of Steel Embedded in Ordinary Portland Cement Concrete. *American Journal of Materials Research.* Vol. 1, No. 4, 2014, pp. 53-58.

Abstract

The effect of Al_2O_3 addition on the corrosion and electrochemical behavior of steel imbedded in ordinary Portland cement concrete was investigated using weight loss method, open-circuit potential measurements (OCP), Tafel polarization and Cyclic polarization techniques. Several mixture proportions were used to produce concrete specimens, where Al_2O_3 particles replaced cement. The internal structure of concrete was investigated by scanning electron microscopy (SEM) and X-ray diffraction (XRD). Concrete specimens were exposed to 3.5 wt.% NaCl solution. It was concluded that Al_2O_3 addition improves the corrosion resistance and the 5wt. % addition as a cement replacement shows the optimum value. When Al_2O_3 is added in greater percentages the corrosion resistance decreases but still more than plain concrete.

1. Introduction

Reinforced concrete is the most commonly used composite material in structural practices due to ease in applications and lower cost of construction. Besides, reinforced concrete structures offer good service under certain environmental conditions [1-3]. Corrosion is one the major causes of deterioration of concrete structures [4, 5]. Corrosion not only affects the mechanical properties of steel but the corrosion products induce the stresses in the concrete which easily exceed the limited tensile strength of concrete and cause cracking of concrete and thereby reducing the ultimate strength of concrete elements in structures, decreasing the bond strength and hence reducing the service life of the structures [6]. By nature, the high alkalinity of the concrete pore solution (pH13) provides protection to the reinforcing steel but the penetration of carbon dioxide CO_2 decreases the pH from 13 to 9, causing general corrosion. Moreover, chloride ions can as well break down the passive layer and cause the mix of general and pitting corrosions. Usually, the layer of corrosion products consists of liquid water and hydrated iron oxides. Due to volume expansion of the oxides, the cracking of concrete leads to a dangerous fall of concrete parts and to unprotected steel [7,8]. The worldwide demand for high performance concrete with improved corrosion resistance has increased and it is expected that it will be widely used in construction industry during next decades [1].

The development and use of blended cement is growing rapidly in the construction industry mainly due to considerations of cost saving, energy saving, environmental protection and conservation of resources [9]. The use of mineral admixtures such as silica fume, fly ash and granulated blast furnace slag in the concrete production has gained prominence in global concrete construction [10]. Previous studies reported that the use of pozzolanic material in blended cement paste can reduce pore sizes and average pore diameters, leading to good resistance against chloride ingress and steel corrosion [11–17].

In this study, reinforced concrete samples were produced with mineral admixtures replacing cement. Al_2O_3 has replaced cement as mineral admixture at the ratios of 2.5, 5, 10, and 15 wt. %. The corrosion and electrochemical tests have been conducted in 3.5 wt. % NaCl solution.

2. Materials

The present study was performed using a commercial Portland type CEM I 42.5 N meeting the requirements of BS EN 197-1:2000. Al_2O_3 admixture was delivered in 250-g package with particle size 50 µm. Aggregates: natural siliceous sand having a fineness modulus of 2.66 and a specific gravity of 2.67 was used. Crushed dolomite with a maximum nominal size of 18 mm was used as coarse aggregate. The aggregate had a specific gravity of 2.64 and a crushing modulus of 23 percent. High tensile ribbed steel bars of 9 mm diameter were cut into 15 cm. The water used was clean, fresh, free from impurities, and was taken from portable water supplies. The concrete composition used in the experimental program was as follows: 1/3 cements / aggregate with water/cement ratio of 0.5.

All solutions were freshly prepared from analytical grade chemical reagents using distilled water.

2.1. Preparation of Test Specimen

To disperse Al_2O_3 additives uniformly they were added into water and stirred at high speed. The sand and gravel were placed in the mixer and started mixing. Then the cementitious materials were added to the mixer and stirred for 2 min. The mixing water was slowly added and mixed for 2 min. Mixing was continued for 5 min; the mixer stopped for 3 min, and then continued mixing for an additional 2 min. Upon completion of mixing, the fresh concrete were placed into the molds to form the cubes of size 15×15×15 cm for all mixing proportion and tests (see Fig.1). The steel bars were cleaned with ethanol and then dried prior to embedding in the center of concrete. After 24 hours, the specimens were demoulded and cured in water for 28 days. Each water-cured cube was taken from water at each of the test age and then rubbed with a clean dry cloth until a saturated surface dry sample was obtained.

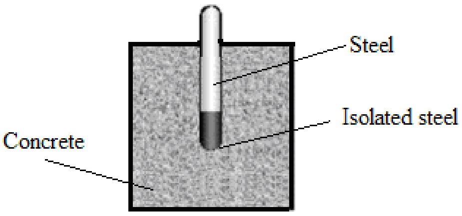

Fig. 1. *Reinforced concrete specimen.*

2.2. Weight Loss Method

Static immersion corrosion tests were carried out at room temperature according to ASTM G1 and G31 [18]. Concrete cubes of size 15×15×15 cm were cast with partial replacement of Al_2O_3 by the weight of cement at 2.5, 5, 10 and 15 wt.%. High tensile ribbed steel bars was embedded at a cover of 25 mm in the cube. Initially the steel bars were cleaned in HCl acid solution for 5 minutes, degreased with acetone and washed with distilled water and dried. The initial weight of the steel bars was taken before casting using an analytical balance for the original weight (W_0). After immersion in 3.5 wt.% NaCl solution for 15 days , At the end of the exposure period, the concrete specimens were broken and the rebar specimens were removed and cleaned with HNO_3 solution for 3 min and dried. After cleaning, the specimens were reweighed and the loss in weight was calculated. From the weight loss values, the corrosion rates were obtained from the relationship:

The corrosion rate CR (from the mass loss) was calculated using the following equation [18]:

$$CR = \frac{K \cdot W}{A \cdot D \cdot T} \tag{1}$$

where CR is the corrosion rate expressed in mils per year (mpy), K is a constant (3.45×10^6), T is the time of exposure (h), A is the area (cm^2), W is the weight loss in the nearest 1 mg and D is the density of the material (g/cm^3).

2.3. Electrochemical Technique

All electrochemical experiments were conducted with a Potentiostat/ Galvanostat (EG&G model 273). M352 corrosion software from EG&G Princeton Applied Research was used. A three-electrode cell composed of a concrete specimen as a working electrode, Pt counter electrode, and Ag/AgCl reference electrode were used for the tests (see Fig.2).

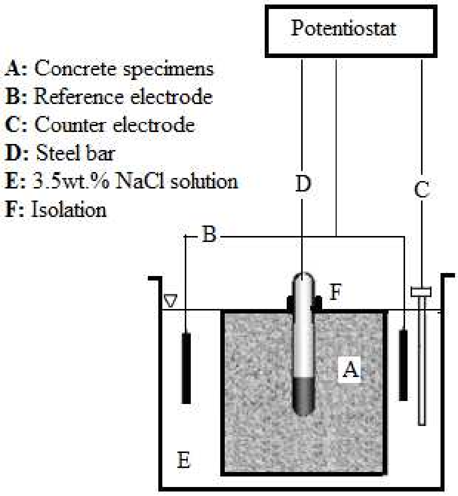

Fig. 2. *Experimental setup for electrochemical corrosion measurement.*

The open-circuit potential (OCP) was recorded after immersion of the samples in the test solution for 60 days vs. Ag/AgCl reference electrode.

Tafel polarization tests were carried out at a scan rate of 0.5 mV/min.The PAR Calc Tafel Analysis routine statistically fits the experimental data to the Stern-Geary model for a corroding system. The routine automatically selects the data that lies within the Tafel region (±250 mV with respect to the corrosion potential). It then calculates the corrosion current and the corrosion rate.

The cyclic potentiodynamic curves were obtained by scanning the potential in the forward direction from -1200 mV Ag/AgCl towards the anodic direction at a scan rate of 2.0 mV/s. The potential scan was reversed in the backward direction when the current density reached a value of 0.10 A/cm^2. At least three separate experiments were carried out for each run to ensure reproducibility of results. After cyclic polarization measurements, all specimens were taken out and dried.

2.4. Surface Analysis

The analysis of the microstructure of a concrete yields several information regarding phase identification, presence of voids, etc. In the present work, X-ray diffraction (XRD, Philips Analytical X-ray B.V. Machine) and scanning electron microscope (SEM, Joel-JXA-840A) have been used to observe the microstructure of concrete with and without mineral admixtures. Moreover, the surface of steel bars after corrosion tests was analyzed by scanning electron microscope. All samples were coated with gold to improve the appearance of microstructure.

3. Results and Discussions

3.1. XRD Analysis

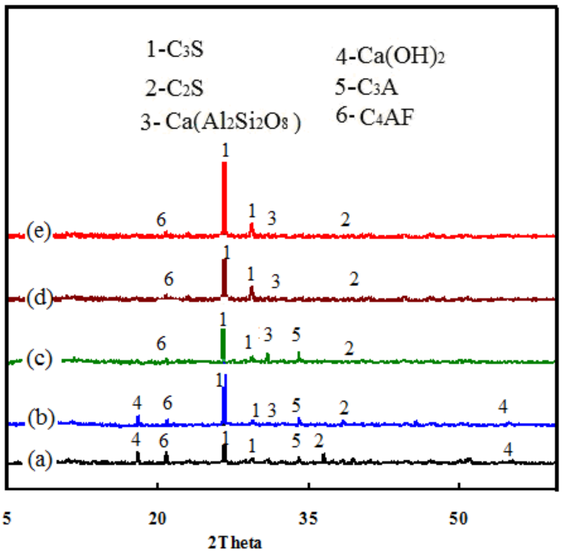

Fig. 3. XRD diffraction of concrete with and without Al_2O_3 additives. (a)-concrete without additives, (b)-2.5wt.% Al_2O_3, (c)-5 wt.% Al_2O_3,(c)- 10wt.% Al_2O_3 and (e)- 15 wt.% Al_2O_3

To explain the effect of Al_2O_3 additives on corrosion and electrochemical behavior of steel imbedded in concrete, the internal structure of concrete with and without Al_2O_3 particles was examined by XRD and SEM analysis at 28 days.

Fig. 3(a-e) shows, XRD of concrete with and without Al_2O_3. The internal structure of plain concrete mainly consists of C_3S and $Ca(OH)_2$ while the minor phases are C_2S, $Ca(Al_2Si_2O_8)$ and Ca_4AF. The same structure was also observed for concrete with 2.5 wt. % Al_2O_3. On the other hand Fig. 3(a-e) indicates that increasing Al_2O_3 contents from 2.5 to 15 wt. %, the main phases of internal structure are similar.

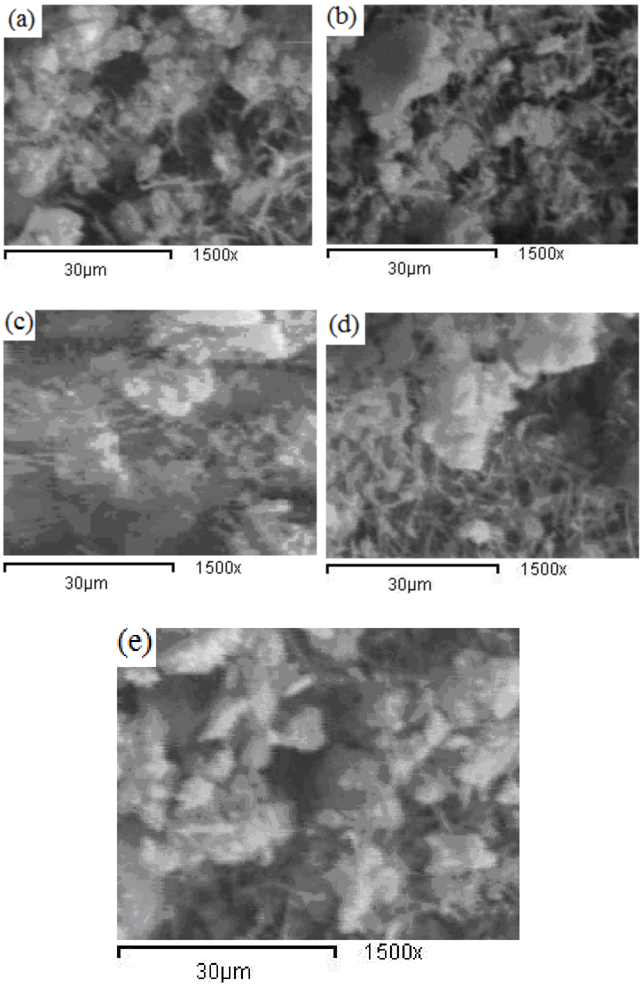

Fig. 4. Microstructure of concrete with and without Al_2O_3 additives. (a)-concrete without additives, (b)- 2.5wt.% Al_2O_3, (c)- 5 wt.% Al_2O_3,(c)-10wt.% Al_2O_3 and (e)- 15 wt.% Al_2O_3

Fig. 4(a) shows, the ordinary Portland cement concrete without Al_2O_3 additives. It has independently formed a C-S-H gel, mutually linked needle-shaped hydrates (ettringite), and many $Ca(OH)_2$ crystals, showing a sparse internal structure with non-crystal hydrates. Fig. 4(b) shows the structure of concrete with 2.5 wt. % Al_2O_3. It can be seen that the internal structure of 2.5 wt. % Al_2O_3 concrete was similar to the structure of Portland cement concrete without Al_2O_3 additives but it has small pore size. As seen in Fig. 4(c-e) the quantity of hydration products derived from the concretes produced by 5,10 and 15 wt. % Al_2O_3 admixtures is low compared to 0.0 and 2.5 wt. % Al_2O_3 concrete types. However, a denser formation of hydration products for 5 wt. % Al_2O_3 was observed.

3.1.1. Immersion Tests

The corrosion rate of steel imbedded in concrete with and without Al_2O_3 additives was studied by weight loss method in 3.5 wt. % NaCl solution. Fig.5 shows that with increasing the Al_2O_3 content to 5 wt. %, the corrosion rate decreases. This may be due to specimens of 0.0 and 2.5 wt. % Al_2O_3 contains $Ca(OH)_2$ which have divers effect on concrete. While increasing Al_2O_3 content more than 2.5 wt. %, all $Ca(OH)_2$ molecules which are produced during hydration of cement reacts with Al_2O_3 and forms CSH. When the amount of Al_2O_3 goes beyond 5 wt. %, the Al_2O_3 particles agglomerate and increase the voids in concrete. Hence, the microstructure of 5 wt. % Al_2O_3 concrete was denser than other type.

3.1.2. Open Circuit Potential (OCP)

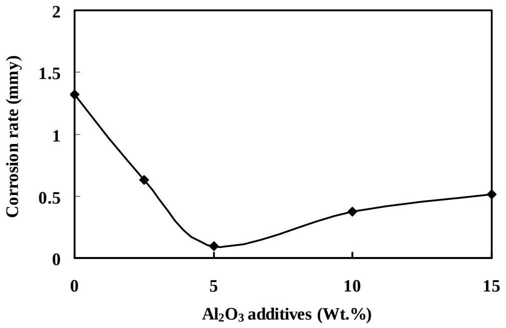

Fig. 5. *Effect of Al_2O_3 additives on the corrosion rate of steel imbedded in concrete in 3.5wt. % NaCl solution using weight loss method*

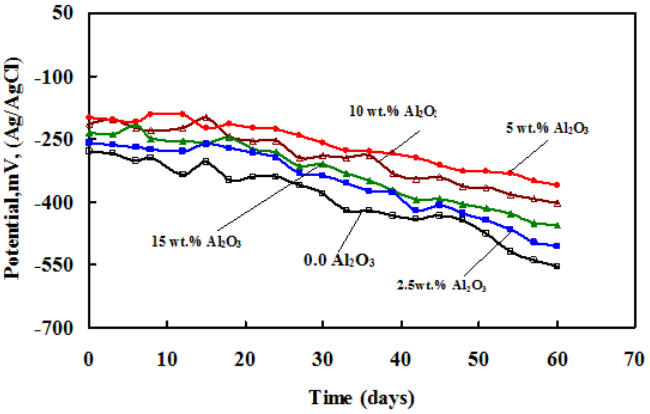

Fig. 6. *Potential–time curves of steel imbedded in concrete with and without Al_2O_3 additives in 3.5 wt. % NaCl solution*

Steel in concrete structures is normally protected from corrosion by a passive film due to the high alkalinity of the concrete. However, in presence of water and oxygen together with a sufficient amount of chlorides and/or carbon dioxide, this film can be destroyed and corrosion occurs. In order to investigate the behavior of the passive film on the steel surface in presence of Al_2O_3 additives, the open circuit potential (OCP) with time was used. Fig. 6 indicates the OCP with time. The recorded results reveal that the corrosion potential of steel embedded in control concrete showed negative potential more than steel in concrete with Al_2O_3 additives. Moreover, Fig. 6 indicates that increasing Al_2O_3 contents from 2.5 to 5 wt. % the OCP shifts to more positive values. When the amount of Al_2O_3 goes beyond 5 wt. %, the OCP shifts to negative direction. These results indicated that steel embedded in ordinary Portland cement concrete up to 5% Al_2O_3 performed better than the other conditions. This behavior may be attributed to Al_2O_3 is supposed to react with free lime in concrete and forms $CaAl_2Si_3O_{12}$, which in turn reduces the permeability of chloride and improves the corrosion resistance property of embedded steel in concrete. On the other increasing Al_2O_3 more than 2.5 wt. % postpones the reaction with free lime. This explanation was supported by X-ray results (Fig 3). Similarly, Thangavel et al. [19] examined the effect of Al_2O_3 content on the corrosion resistance of steel imbedded in concrete by OCP with time. They observed that steel embedded in OPC control concrete showed active condition within 6 cycles of exposure. On the other hand, OPC with various levels up to 5% maintained its passive condition of embedded steel throughout the exposure period of 12 months. However, OPC with 10% and 15% Al $_2O_3$ levels showed active condition within 4 cycles of exposure.

3.1.3. Tafel Polarization

Fig. 7 shows Tafel polarization curves of steel imbedded in concrete with and without Al_2O_3 additives in 3.5 wt. % NaCl solution. All the samples were immersed in 3.5 wt. % NaCl solution for about 15 days before polarization tests to achieve their stable OCP values. It can be seen that the cathodic current densities increased with increasing Al_2O_3 additives. The cathodic reaction is oxygen reduction.

$$2O_2 + H_2O + 2e^- = 2OH^- \tag{2}$$

The anodic polarization curves showed that with increasing Al_2O_3 additives to 5 wt. %, the corrosion potential (E_{cor}) shifted to more noble potential and the corrosion rate decreased from 1.128 to 0.076 mmy. Increasing the amount of Al_2O_3 beyond 5 wt. % decreased the corrosion resistance of steel in concrete. The partial anodic reaction occurring at anodic sites is:

$$Fe \rightarrow Fe^{+2} + 2e \tag{3}$$

The released electrons from anode can support the cathodic reaction. When chloride and sodium ions exist in solution, the cathode product is sodium hydroxide, and the anode product is ferric chloride. Ferric hydroxide is oxidized into ferric iron (FeO-OH or Fe_2O_3 H_2O), and corrosion current intensity largely depends on the amount of oxygen delivered to the cathode. If the cathode reactants wrap large size of the area, the anode current becomes greater, and makes serious corrosion of steel rebar [8].

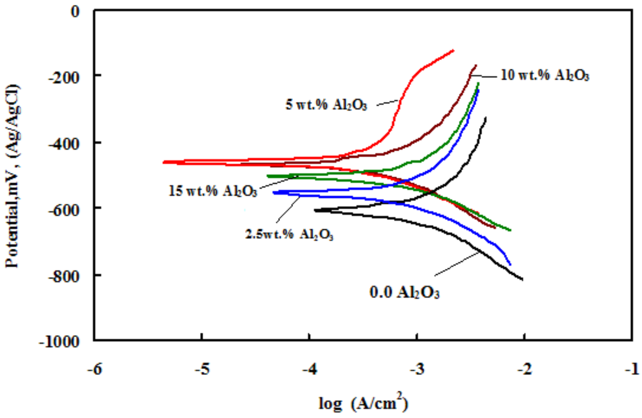

Fig. 7. *Tafel polarization curves of steel imbedded in concrete with and without Al_2O_3 additives in 3.5 wt. % NaCl solution*

The electrochemical parameters including corrosion potential (E_{corr}), corrosion current density (i_{corr}), corrosion rate, anodic and cathodic slopes (β_a and β_c) were calculated from Tafel plots, and are summarized in Table 1.

Table 1. *Corrosion parameters of steel imbedded in concrete with and without Al_2O_3 additives in 3.5 wt. % NaCl solution*

Al_2O_3, wt. %	$E_{cor.}$ (mV)	i_{cor}(A/cm^2)	mmy	β_c (mV/dec)	β_a (mV/dec)
0.0	-610	986.4×10^{-6}	1.128	154.3	232.5
2.5	-555	455.7×10^{-6}	0.521	86.4	122.6
5.0	-460	66.52×10^{-6}	0.076	66.4	85.0
10	-470	277.5×10^{-6}	0.317	85.7	117.4
15	-505	355.7×10^{-6}	0.407	91.9	127.6

It can be seen from Table 1 that the anodic and cathodic Tafel slopes were changed with increasing Al_2O_3 additives. This means that Al_2O_3 admixture affects on anodic and cathodic reaction.

3.1.4. Cyclic Polarization

Chloride ions can penetrate the pores in concrete and attack the passive film on the steel surface and cause pitting corrosion, even in a high pH environment. In order to investigate the effect of Al_2O_3 additives on passive stability and pitting of steel imbedded in concrete contaminated with chloride ions, the cyclic polarization technique was used. Two pitting parameters are determined from cyclic polarization curve: pitting potential E_{pit} and protection potential E_{prot}, E_{pit} denotes the potential at which pits initiate on the forward scan and the current increases abruptly. E_{prot} is the potential at which the pits are repassivated during the reverse scan, and the current decreases and reaches the passive current density value. Fig. 8 indicates the cyclic polarization curves of steel imbedded in concrete with and without Al_2O_3 additives in 3.5 wt. % NaCl solution. It is obvious from Fig. 8 that the obtained plots had the familiar form for steel in concrete showing a well-defined corrosion potential, E_{corr}, followed by a passive region. The passive region results due to the formation of a protective barrier oxide film which is related to the structure of the passive film. On the other hand Fig. 8 indicates that the passive region increases with increasing Al_2O_3 additives to 5 wt.%. When Al_2O_3 is added in greater percentages there is no positive effect on the passivity of steel in concrete. Moreover, the reverse anodic curves are shifted to lower currents (negative hysteresis) and hence no pitting is expected for all concrete specimens with and without Al_2O_3 additives.

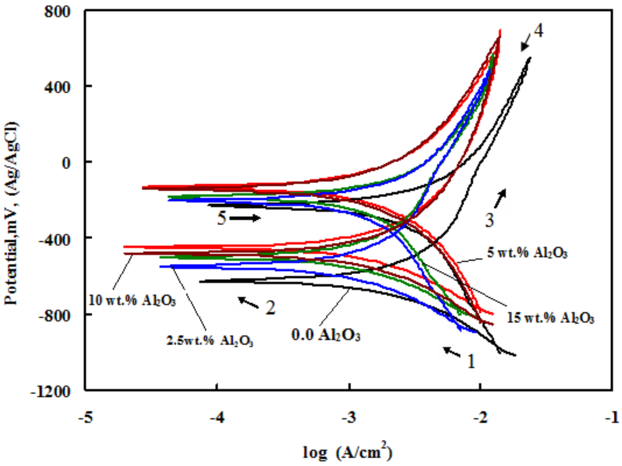

Fig. 8. *Cyclic polarization curves of steel imbedded in concrete with and without Al_2O_3 additives in 3.5 wt. % NaCl solution*

4. Conclusions

Based on the results obtained, it can be concluded that Al_2O_3 addition improves the corrosion resistance and the 5wt. % addition as a cement replacement shows the optimum value. When Al_2O_3 is added in greater percentages the corrosion resistance decreases but still more than plain concrete.

References

[1] E.Güneyisi, M. Gesoglu, F. Karabog, K. Mermerdas.Corrosion behavior of reinforcing steel embedded in chloride contaminated concretes with and without metakaolin. Composites: Part B 45 (2013) 1288–1295.

[2] I.Turkmen, M. Gavgali ,R. Gul. Influence of mineral admixtures on the mechanical properties and corrosion of steel embedded in high strength concrete. Materials Letters 57 (2003) 2037– 2043.

[3] Y.M. Tang, Y.F. Miao, Y. Zuo , G.D. Zhang, C.L. Wang. Corrosion behavior of steel in simulated concrete pore solutions treated with calcium silicate hydrates. Construction and Building Materials 30 (2012) 252–256.

[4] V. Saraswathy , H.W. Song. Electrochemical studies on the corrosion performance of steel embedded in activated fly ash blended concrete. Electrochimica Acta 51 (2006) 4601–4611.

[5] H. Binici, O. Aksogan, M.Y. Durgun. Corrosion of basaltic pumice, colemanite, barite and blast furnace slag coated rebars in concretes. Construction and Building Materials 37 (2012) 629–637.

[6] I. Khan, R. François , A. CastelMechanical behavior of long-term corroded reinforced concrete beam. Proceedings of the Joint fib-RILEM Workshop held in Madrid, Spain,22–23 Nov. (2010) 243-259.

[7] A. Ouglova, Y. Berthaud, M. Franc¸ois, F. Foct. Mechanical properties of an iron oxide formed. Corrosion Science 48 (2006) 3988–4000.

[8] M. M. Sadawy, M. T. Nooman, E. R. Elsharkawy.Formation and characterization of zinc phosphate coating on reinforcing steel rebars. Journal of Materials Science and Engineering A 3 (7) (2013) 481-487.

[9] V. Saraswathy, H.W. Song. Electrochemical studies on the corrosion performance of steel embedded in activated fly ash blended concrete. Electrochimica Acta 51 (2006) 4601–4611.

[10] I. B.Topçu, T. Uygunoglu, I. Hocaoglu. Electrical conductivity of setting cement paste with different mineral admixtures. Construction and Building Materials 28 (2012) 414–420.

[11] W. Chalee, T. Sasakul, P. Suwanmaneechot , C. Jaturapitakkul. Utilization of rice husk barks ash to improve the corrosion resistance of concrete under 5-year exposure in a marine environment. Cement & Concrete Composites 37 (2013) 47–53.

[12] P. Chindaprasirt, C. Jaturapitakkul, T. Sinsiri. Effect of fly ash fineness on compressive strength and pore size of blended cement paste. Cement & Concrete Composites 27 (2005) 425–428.

[13] C Andrade, Renata Bujak. Effects of some mineral additions to Portland cement on reinforcement corrosion. Cement and Concrete Research 53 (2013) 59–67.

[14] O. Kelestemur, B. Demirel, Corrosion behavior of reinforcing steel embedded in concrete produced with finely ground pumice and silica fume. Construction and Building Materials 24 (2010) 1898–1905.

[15] K.Y. Ann, T.-S. Kim, J.H. Kim, S.-H. Kim. The resistance of high alumina cement against corrosion of steel in concrete. Construction and Building Materials 24 (2010) 1502–1510.

[16] P. Chindaprasirt, S. Rukzon. Strength, porosity and corrosion resistance of ternary blend Portland cement, rice husk ash and fly ash mortar. Construction and Building Materials 22 (2008) 1601–1606.

[17] P. Chindaprasirt, C. Chotithanorm, H.T. Cao, V. Sirivivatnanon. Influence of fly ash fineness on the chloride penetration of concrete. Construction and Building Materials 21 (2007) 356–361.

[18] ASTM Standard G1 and G31, ASTM International, West Conshohocken, PA, 1994.

[19] K. Thangavel, S. Muralidharan, V. Saraswathy. Relationship between alumina and chloride content on their physical and corrosion resistance properties of concrete. The Arabian Journal for Science and Engineering, 35, 2B (2010) 27-38.